A Chitosan Hydrochloride Mediated, Simple and Efficient Approach for the Synthesis of Hydrazones, their *in vitro* Antimycobacterial Evaluations, and Molecular Modeling Studies (Part III)

Suraj N. Mali[*a]
Anima Pandey[*a]
Bapu Thorat[b]

[a] Department of Pharmaceutical Sciences and Technology, Birla Institute of Technology, Mesra, Jharkhand-835215, India
Mali.suraj1695@gmail.com
apandey@bitmesra.ac.in
[b] Department of Chemistry, Government College of Arts and Science, Aurangabad, MS – 431001, India

This article is dedicated to my lovely parents, and my younger brother Sagar Mali, who deep-heartedly supported me to achieve my goals

Published as part of the Virtual Collection
Click Chemistry and Drug Discovery

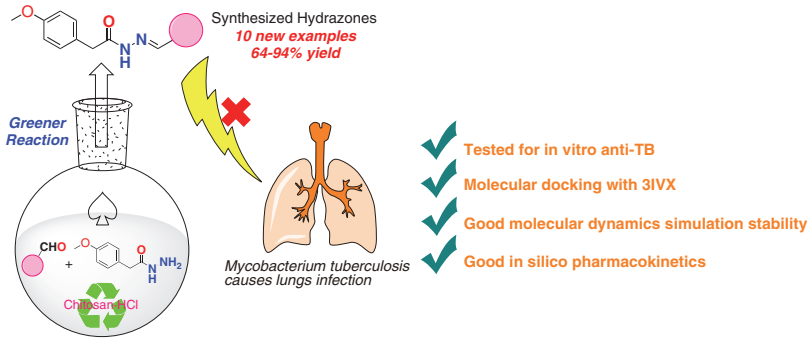

Received: 16.01.2023
Accepted after revision: 14.02.2023
Published online: 14.02.2023 (Accepted Manuscript), 07.03.2023 (Version of Record)
DOI: 10.1055/a-2035-6493; Art ID: SO-2023-01-0005-OP

Abstract A simple, eco-friendly and straightforward synthesis of hydrazones has been devised that is conducted in the presence of chitosan Hydrochloride (chitosan·HCl) as catalyst in aqueous-ethanol medium at room temperature. The current protocol offers metal-free synthesis, adaptability to large-scaleup, good yields, and quicker reaction time. All ten synthesized hydrazones also showed good antimycobacterial activity, with minimum inhibitory concentrations (MICs) ranging from 3.12 to 6.25 µg/mL. One of the products presented strong binding affinity against *M. tuberculosis* pantothenate synthetase (pdb id: 3IVX) with a Glide docking score of –8.803 kcal/mol. Molecular dynamics simulation analysis of its complex with 3IVX retained good stability over the simulation period of 20 ns.

Key words carbonyl compounds, green and sustainable chemistry, hydrazides, hydrazones, chitosan hydrochloride, metal-free synthesis

Hydrazide–hydrazones are chemical moieties that contain an azomethine group (–NH–N=CH–) connected with a (-C=O-) carbonyl group.[1–3] They attract continuing interest due to their wide spectrum of pharmacological activities. Compounds bearing such moieties were reported to have a number of bioactivities including anti-inflammatory, analgesic, anticancer, anticonvulsant, EGFR inhibitory, antiprotozoal, and antiviral action.[1–3] However, this class of compound is most commonly reported as antimicrobial agents.[2] It is also impressive to note that the hydrazide–hydrazone moiety is also present in the chemical structure of drugs with antimicrobial activity, such as nitrofurazone, furazolidone, and nitrofurantoin.[4–28]

A typical synthesis of hydrazone involves a condensation reaction between a carbonyl compound and a hydrazide, requiring a dehydrating agent.[29] The use of various acid catalysts such as polystyrene sulfonic acid, glacial acetic acid, choline chloride–oxalic acid, or meglumine, have been reported.[29–38] Although these protocols are effective in many cases for the synthesis of hydrazone derivatives, some of them have one or more drawbacks, such as the use of volatile organic solvents, unsatisfactory yields, over-oxidization of aldehydes to carboxylic acids, long reaction times, high temperatures, difficulties in product isolation, lack of generality, or the need for special apparatus.[39] Many protecting groups, in particular, are rapidly deprotected under acidic environments. As a result, the development of a more efficient process for synthesizing hydrazone derivatives under environmentally friendly conditions remains extremely desirable.[39] In our previous report, we described the use of chitosan hydrochloride to synthesize a new set of hydrazones.[40]

Moreover, from our previous medicinal chemistry knowledge[41–49] on hydrazones as antitubercular agents (anti-TB) agents, we noticed that these moieties presented particularly strong anti-TB activities, with typical minimum inhibitory concentrations (MICs) ranging from 1.25 to 100 µg/mL. In a continuation of this study, we further extended our work to synthesize a set of hydrazones with chitosan hydrochloride as a catalyst.[40] All synthesized hydrazones were also assessed for their probable binding modes against *Mycobacterium tuberculosis pantothenate synthetase* using molecular docking analysis.[41,43] Further, the best docked

compound was also subjected to molecular dynamics analysis to establish the binding stability against the selected target (pdb id: 3IVX). Finally, we calculated in silico ADMET (absorption, distribution, metabolism, excretion, and toxicity) properties to gain a better understanding of the probable pharmacokinetics and toxicities.

To understand the reaction optimizations and their relevant parameters, we used the model reaction 1 [benzaldehyde (1 mmol) and phenylhydrazine (1 mmol); Table 1, entry 1]. For catalyst screening, we used previously reported reaction solvent,[39] aqueous ethanol (water/ethanol, 1:1, v/v). The reaction was carried out at room temperature (27 °C). We had noted that the model reaction with no catalyst yielded 48% product, (*E*)-1-benzylidene-2-phenylhydrazine after 60 min reaction time.[39] As presented in Table 1, for various catalysts (entries 2–7), yields ranging from 48 to 90% were achieved after 60 min reaction time.[39] In addition, we observed that the reaction time could be reduced with the use of chitosan HCl as a catalyst (27 °C, 60 min, 93% yield; Table 1). Thus, we extended the use of chitosan HCl to the reaction shown in Scheme 1. The catalyst was prepared as per the reported procedure.[40] Surprisingly, the reaction proceeded smoothly in water/ethanol (1:1, v/v) at room temperature with higher yields >93%.[39] Formation of the imine (Schiff base or hydrazone) took place reversibly at slightly acidic pH (5.5–6.5). The reaction did not reach completion when it was carried out without catalyst, so the yield obtained in the absence of catalyst was about 48%. The use of mannitol and meglumine as catalysts was previously reported for imine bond formation in aqueous ethanol. Both these compounds are weakly alkali in aqueous ethanol, which leads to irreversible dehydration of the tetrahedral intermediate. Chitosan hydrochloride maintains acidic pH in aqueous ethanol (liberate free HCl in aqueous ethanol) and favors the formation of hydrazone, which is not possible in pure organic solvent such as dichloromethane, methanol, or absolute ethanol. Chitosan is a polymeric material so it is not soluble in pure dichloromethane, methanol, or pure ethanol, but its hydrochloride (15 wt%) liberates trace amounts of HCl in aqueous ethanol, which was sufficient for hydrazone formation.

The variation of yield may be explained by the polarity of the solvent, which is determined by the amount of free HCl liberated from chitosan·HCl. We found that an increase in temperature for our newly optimized reaction had no significant effect on the product yield. However, a reduction in time required for reaction completion from 15 to 10 minutes was observed. Taking account of environmental considerations, this reaction can also be carried out using water/ethanol (1:1, v/v) as solvent at room temperature. From Table 2, we can also see the effects of various solvents and catalytic loading of chitosan HCl for model reaction 1 (shown in Table 1). The reaction using EtOH and water gave the corresponding product (*E*)-1-benzylidene-2-phenylhydrazine in higher yields than with glycerin (Table 2, entries 3 and 4), while the results with other solvents such as CH_2Cl_2, and polyethylene glycol (PEG) 400 were not satisfactory.[39] Our further analysis demonstrated that the best choice of solvent system was aqueous ethanol (water/ethanol, 1:1, v/v) (entries 6 and 7), and that the yield of product was higher with a catalytic load of 15 wt% than with 10 wt%. When the catalytic amount of chitosan·HCl was increased to 20 wt% a yield of final product of 93% was achieved after 15 minutes reaction. Finally, the catalytic load of chitosan·HCl 20 wt% was kept constant for optimization of the reaction shown in Scheme 1, with a solvent system of aqueous ethanol (water/ethanol, 1:1, v/v) at room temperature.

Table 1 Initial Optimization of Reaction Conditions for Various Catalysts[a]

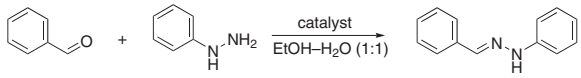

Entry	Catalyst	Temp. (°C)	Time (min)[c]	Yield (%)[d]
1	no catalyst	27	60	48
2	L-proline	27	60	61
3	chitosan	27	60	78
4	meglumine	27	60	90
5	piperidine	27	60	74
6	lipase	27	60	NR[e]
7	mannitol	27	60	72
8 (current work)[a]	Chitosan HCl	27	15	93
9 (current work)[b]	Chitosan HCl	40	10	93

[a] Reaction conditions (model reaction 1): benzaldehyde (1 mmol), phenylhydrazine (1 mmol), catalyst (0.15 mmol), EtOH/H_2O (1:1, 4 mL).
[b] The conditions used in entry 8 were applied to the reaction shown in Scheme 1.
[c] The progress of the reaction was monitored by TLC.
[d] Isolated yield.
[e] No reaction.

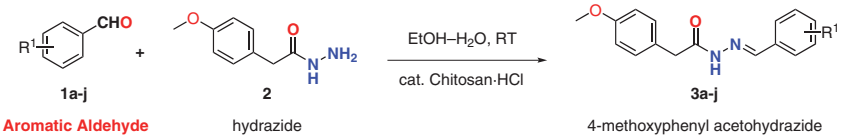

Scheme 1 Synthesis of 4-methoxyphenyl acetohydrazide analogues

Table 2 Initial Optimization of Reaction Conditions with Various Solvents[a]

Entry	Chitosan HCl loading (wt%)	Solvent	Temp. (°C)	Time (min)[c]	Yield (%)[d]
1	15	CH_2Cl_2	27	15	62 (43)[e]
2	15	MeOH	27	15	43 (29)[e]
3	15	EtOH	27	15	55 (39)[e]
4	15	H_2O	27	15	47 (31)[e]
5	15	glycerin	27	15	NR
6	10	EtOH/H_2O (1:1 v/v)	27	15	72
7	15	EtOH/H_2O (1:1 v/v)	27	15	86
8 (current work)[a]	20	EtOH/H_2O (1:1 v/v)	27	15	93
9 (current work)[b]	20	EtOH/H_2O (1:1 v/v)	40	10	93

[a] Reaction conditions (model reaction 1): benzaldehyde (1 mmol), phenylhydrazine (1 mmol), solvent (4 mL).
[b] The optimized condition given in entry 8 was applied for the reaction shown in Scheme 1.
[c] The progress of the reaction was monitored by TLC.
[d] Isolated yield.
[e] Yield obtained with no catalysts loading at same reaction conditions given in parentheses.

As shown in Figure 1, a variety of substituted aromatic aldehydes, irrespective of the presence of electron-donating or electron-withdrawing functional groups attached to the benzene ring, reacted with phenylhydrazine to give the desired products in high to excellent yields.[39] To elaborate the reaction scope of the model reaction 1 (Table 1), we additionally varied the aldehydes with the same catalyst system (see the Supporting Information). Encouraged by these results, we next applied this protocol to the reaction shown in Scheme 1 with a range of aromatic aldehydes (**1a–j**). Without any further optimization, we were pleased to see good yields of final products **3a–j** (Figure 1). The underlying reaction mechanism for this reaction catalyzed by chitosan·HCl is depicted in Figure 2.

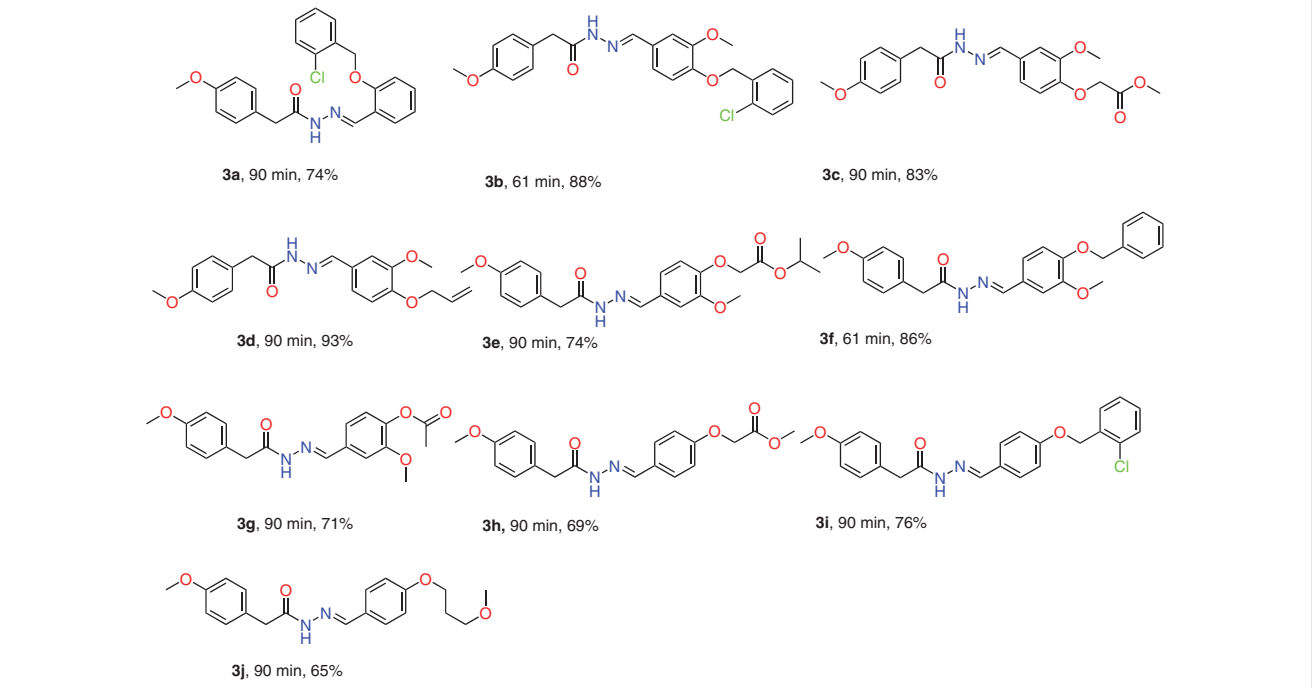

Figure 1 Reaction scope

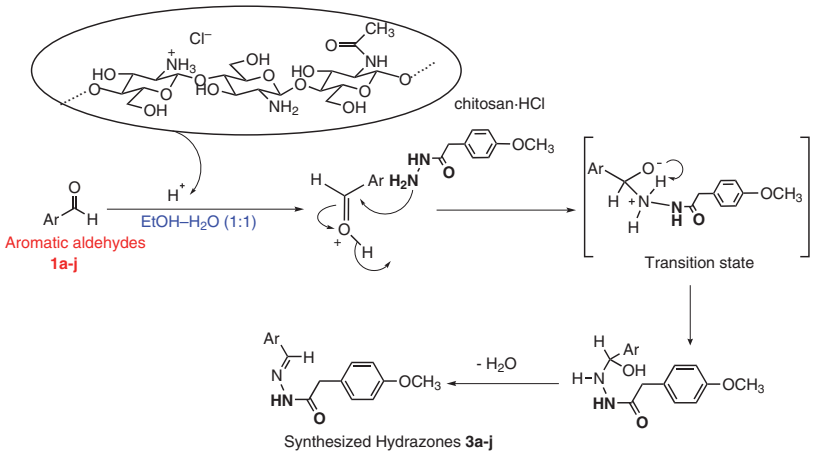

Figure 2 Reaction mechanism

In vitro Antimycobacterial Activity

In vitro antimycobacterial activity was assessed by using a microplate Alamar Blue assay (MABA)[43] against *Mycobacteria tuberculosis* (Vaccine strain, H37RV strain): ATCC No. 27294 (Figure 3). We recorded minimum inhibitory concentrations (MICs; preventing the color change from blue to pink) with reference to three anti-TB drugs, namely, pyrazinamide, ciprofloxacin and streptomycin, as standard. The results suggested that compounds **3c–e** had lower MICs than other compounds, i.e., 3.12 µg/mL each. The other compounds exhibited MIC values of 6.25 µg/mL. It is important to note that the synthesized hydrazones had MICs that were comparable to those of in vitro anti-TB standard drugs such as pyrazinamide (3.12 µg/mL), ciprofloxacin (3.12 µg/mL) and streptomycin (6.25 µg/mL).[39]

Molecular Docking Analysis

To establish probable binding modes[43–57] of synthesized compounds **3a–j** as antimycobacterial agents, we carried out molecular docking simulations on the target enzyme, *Mycobacterium tuberculosis* pantothenate synthetase (PS) (pdb id: 3IVX, Resolution: 1.73 Å), which includes an internal inbound ligand, FG6 ({2-[(1-benzofuran-2-ylsulfonyl)carbamoyl]-5-methoxy-1*H*-indol-1-yl}acetic acid). It is important to note that this target has a key role in the pathogenicity or virulence of *M. tuberculosis*. Further, from our previous analyses of hydrazones, we concluded that hydrazide-hydrazones had higher docking scores with the PS target, which encouraged us to carry our molecular docking interactions for our newer set of hydrazones **3a–j**. Our molecular docking analysis showed that all compounds had Glide, XP docking scores higher than –6.234 kcal/mol. Among them, compound **3b** had a higher docking score (–8.803 kcal/mol) than those of standards ciprofloxacin (–7.23 kcal/mol) or Isoniazid (–6.93 kcal/mol). Compound **3b** interacted preferentially with GLN 72···(CH_2-O-Ar) (H-bonding interactions); HIE44, SER196, GLY46, HIE47 (charged, positive); while amino acid residues ASN69, PHE67, SER65, and GLN 164 had contributions in the hydrophobic pocket of receptor (Figure 4). ASP161, LYS 160, and GLU159 presented polar interactions with **3b**. The compound with the higher docking energy, **3b**, had also good in vitro anti-TB activity (6.25 µg/mL). Thus, we extended our modeling calculations further for molecular dynamics analysis using Schrodinger's Desmond module, 2022 for the complex **3b**:3IVX.

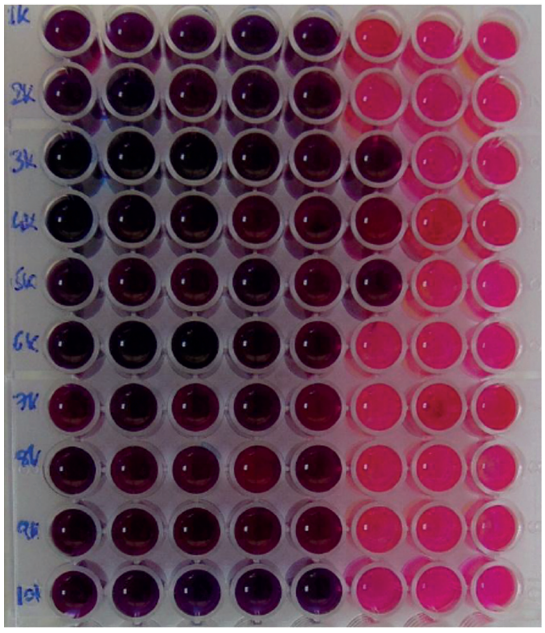

Figure 3 In vitro MABA assay 96-well plate photograph after treatment with compounds **3a–j** (indicated as 1k to 10k, respectively)

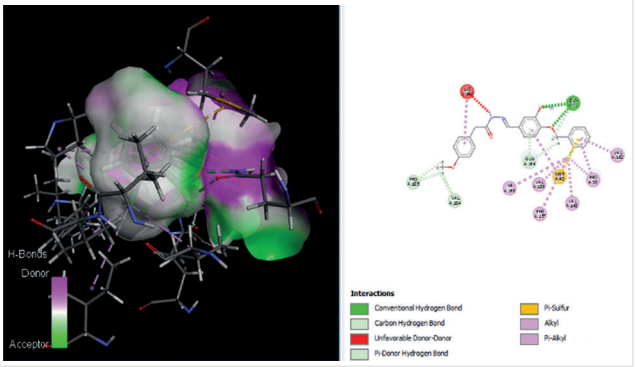

Figure 4 2D- and 3D-interaction diagram of best docked compound **3b** against target PS (pdb id: 3IVX)

Molecular Dynamics (MD) Analysis

We performed MD simulation analysis to establish the stability of the docked molecule **3b** towards the chosen target 3IVX.[55] The total duration of simulation was kept at 20 ns, and the model was comprised of 288 residues of chain A, 4299 atoms, and charge of –4. Ensemble class was kept at NTP mode (Figure 5). In order to see structural changes, trajectory analyses were made for various parameters such as root mean square deviation (RMSD) and root mean square fluctuation (RMSF).

RMSD and RMSF

The backbone changes (N, Cα, C) of the protein were analyzed via RMSD and RMSF evaluations.[55] The protein–ligand RMSD graph shows that the complex has fluctuations over the simulation period of 5 ns and was stabilized after 7.5 ns of simulation time. The protein RMSD value was retained below 2.4 Å, which is generally acceptable and is considered as a good indicator of stability. The RMSF was used to investigate the fluctuation of the complexes as a function of time.[55] The protein RMSF value was also retained below 4.5 Å. The N-terminal had higher fluctuation compared with the C-terminal.

Protein–Ligand Contacts (PLC)

The PLC for analyzed complex **3b**:3IVX suggested that amino acids HIS44, HIS47, GLN72, ASP161 and VAL184 had strong H-bonding interactions, while amino acids PRO38, MET40, ALA49, LEU50, PHE67, VAL139, VAL142, LEU146, and GLN164 presented primarily hydrophobic interactions. Water bridges were also noted for interacting amino acid residues such as HIS44, GLN72, TYR82, GLU128, HIS135, GLY158, ASP161, SER196, SER197, ARG198 and ARG278. It is pertinent to note that ASP161 and VAL187 had the highest percentage of ligand–protein contacts, 95% and 90%, respectively. The conformational evolution of every rotatable bond (RB) in the ligand was also evaluated in the ligand-torsion diagrams.

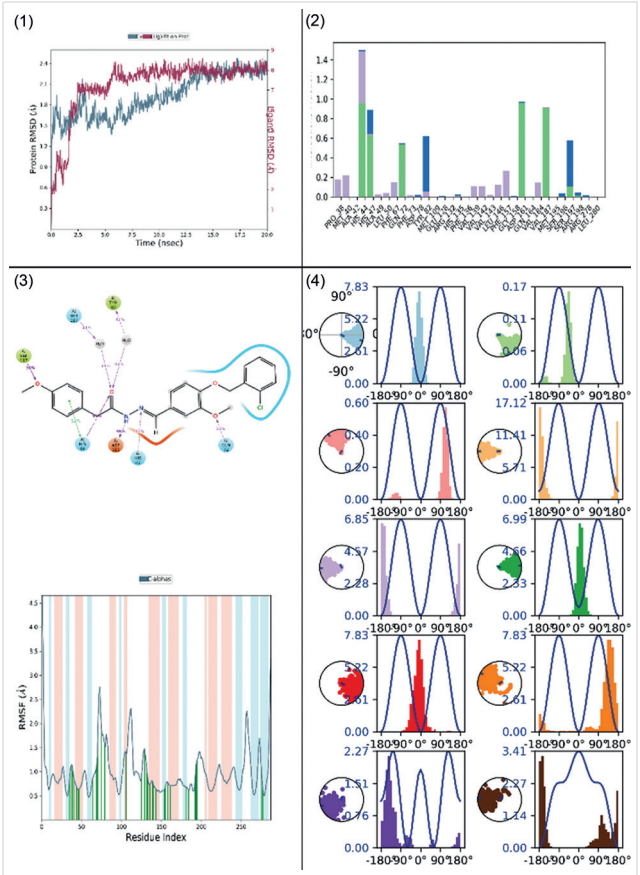

Figure 5 Molecular dynamics simulation plots analyzed for a complex **3b**:3ivx over a period of 20 ns. (1) RMSD and RMSF Graphs for obtained simulation, (2) Ligand interaction Profile, (3) Interaction analysis plot during simulation, (4) Torsion angle analyses

In Silico ADMET (Absorption, Distribution, Metabolism, Excretion and Toxicity) Analysis

Pharmacokinetics plays an important role in the development of safer drugs. Popular Lipinski's Ro5 (Ro5: molecular weight > 500, CLogP >5.0, sum of nitrogen and oxygen (N, O) atoms > 10 and hydrogen bond donors > 5) was developed to set 'drugability' guidelines from an oral bioavailability perspective for small molecules. Considering this rule, we observed no violations of Ro5 for compounds **3a–j**. Furthermore, water-solubility values (LogS) were also determined to be within the range of –3.027 to –3.982 for the hydrazones **3a–j**. For the best docked compound, **3b**, the Acute Oral Toxicity value of 2.031 kg/mol was calculated from the 'admetSAR' server.[56] Compounds, **3b–e** demonstrated higher human oral bioavailability compared to the other compounds. For all compounds, eye corrosion and eye irritations were found to be on the 'negative' side. However, all compounds would likely have 'category III, Acute Oral Toxicity' (Category III has LD_{50} values <500 mg/kg but less than 5000 mg/kg). Other important parameters such as cytochrome 450 enzymes substrate or inhibitions are repre-

sented in the Supporting Information (Tables S1 and S2). As per QikProp calculations, compound **3b** had a QPPCaco permeability of 2654.171 (representing good Caco-2 cell permeability value). Other parameters such as QPlogBB, QPPMDCK, and QPlogHERG, were calculated to be within acceptable limits suggested by QikProp, Schrodinger, LLC, NY, 2022.[57]

To summarize, we have synthesized a set of 10 hydrazones using chitosan·HCl as a catalyst. All compounds shown good anti-TB activity when tested against *Mycobacteria tuberculosis* (Vaccine strain, H37RV strain): ATCC No. 27294. Moreover, compound **3b** had a higher docking score (–8.803 kcal/mol) than other standard drugs such as ciprofloxacin, streptomycin or pyrazinamide. MD simulation analysis of complex **3b**:3ivx demonstrated good stability, as depicted by lower values of RMSD and RMSF. Our in silico analysis also indicates that compounds **3a–j** are likely to exhibit Grade III, Acute Oral Toxicity with no carcinogenicity as calculated from 'admetSAR' server.

The melting point of hydrazones **3a–j** were measured with a digital Optimelt melting-point apparatus and are uncorrected. Fourier-transform infrared (FTIR) spectra were recorded with a Perkin Elmer Tensor-II model, and a Perkin Elmer Lambda-25 double beam spectrophotometer was employed to record absorption data. A Bruker Avance III 500 NMR instrument was used to record the ^{1}H NMR spectra of the final products in $CDCl_3$ using tetramethylsilane (TMS) as an internal reference. Mass spectral data were recorded with a Thermo Scientific, USA (Model: ultimate 3000, LTQ XL) instrument with an electrospray ionization (ESI) source.

Raw chitosan (MW = 50,000–190,000 Dalton) was purchased from Sigma–Aldrich. All compounds were synthesized according to the reported procedures and characterized using spectroscopic techniques (^{1}H NMR, FTIR, etc). Exhaustive details on catalyst characterization and methods are provided in the Supporting Information, and the data is consistent with the reported data.[40] Chitosan hydrochloride (20 wt%) was added to a round-bottom flask containing carbonyl compound (1 mmol) and corresponding hydrazine (1 mmol) in water–ethanol (1:1, 4 mL) as solvent. The reaction, (Scheme 1 and Table 1, model reaction 1**)** was carried out at room temperature, maintaining a stirring rate of 250–300 rpm. The progress of reaction was monitored by TLC (EtOAc/hexane, 9:1). All products were extracted using EtOAc followed by addition of water (5 mL) and EtOAc (5 mL). The organic phase was then dried with sodium sulfate with subsequent removal of organic solvent using a rotary evaporator under vacuum. Crude products were recrystallized (petroleum ether/EtOAc, 1:1) and their melting points, yields and other physical properties were measured.

UV Spectral Analysis and Photoluminescence Study

A detailed description of this analysis is included in the Supporting Information.

(*E*)-1-(3,4-Dimethoxybenzylidene)-2-phenylhydrazine[39]

Yellow solid; mp 136–138 °C.

(1*E*,2*E*)-1,2-Bis(4-fluorobenzylidene)hydrazine[58]

Yield: 96%; yellow crystalline solid; mp 75–78 °C.

(1*E*,2*E*)-1,2-Bis(3-nitrobenzylidene)hydrazine[58]

Yield: 94%; yellow solid; mp 198 °C (lit.[58] 196–197 °C).

4-Methoxyphenyl Acetohydrazide (2)

Yield: 0.92 mmol (93%).

FTIR (neat): 3338, 3302, 3203, 3036, 1642, 1610, 1585, 1508, 1467, 1441, 1340, 1300, 1235, 1184, 1104, 1031, 1006, 966, 919, 860, 820, 794, 729, 712, 668 cm^{-1}.

(*E*)-N′-(2-((2-Chlorobenzyl)oxy)benzylidene)-2-(4-methoxyphenyl)acetohydrazide (3a)

Yield: 0.78 mmol (74%); white solid; mp 153–155 °C; R_f 0.65.

FTIR (neat): 3070, 2898, 1666, 1607, 1508, 1486, 1453, 1436, 1386, 1352, 1297, 1246, 1176, 1145, 1123, 1104, 1035, 948, 932, 906, 811, 776, 758, 746, 714, 701, 683 cm^{-1}.

^{1}H NMR (300 MHz, $CDCl_3$): δ = 8.997 (bs, NH), 8.315 (s, CH=N), 7.975–7.949 (d, 1 H, Ar-H), 7.501–7.226 (m, 7 H, Ar-H), 7.079–6.823 (m, 4 H, Ar-H), 5.214 (s, 2 H, O-CH_2-Ar), 4.020 (s, 2 H, CO-CH_2-Ar), 3.762 (s, 3 H, OCH_3).

Anal. Calcd. for $C_{23}H_{21}ClN_2O_3$: C, 67.56; H, 5.18; N, 6.85; O, 11.74. Found: C, 63.52; H, 5.11; N, 6.72; O, 11.70.

(*E*)-*N*′-(4-((2-Chlorobenzyl)oxy)-3-methoxybenzylidene)-2-(4-methoxyphenyl)acetohydrazide (3b)

Yield: 0.87 mmol (88%); white solid; mp 167–169 °C; R_f 0.72.

FTIR (neat): 3037, 2833, 1650, 1606, 1564, 1510, 1461, 1421, 1382, 1318, 1267, 1245, 1227, 1201, 1167, 1142, 1105, 1058, 1033, 1006, 957, 865, 818, 747, 696, 627 cm^{-1}.

^{1}H NMR (300 MHz, $CDCl_3$): δ = 9.250 (bs, NH), 7.860 (s, CH=N), 7.660–7.337 (m, 8 H, Ar-H), 7.315–6.815 (m, 3 H, Ar-H), 5.298 (s, 2 H, O-CH_2-Ar), 4.028 (s, 2 H, CO-CH_2-Ar), 3.998 (s, 3 H, OCH_3), 3.872 (s, 3 H, OCH_3).

Anal. Calcd. for $C_{24}H_{23}ClN_2O_4$: C, 65.68; H, 5.28; N, 6.38; O, 14.58. Found: C, 63.61; H, 5.22; N, 6.32; O, 13.64.

Methyl (*E*)-2-(2-Methoxy-4-((2-(2-(4-methoxyphenyl)acetyl)hydrazono)methyl)phenoxy)acetate (3c)

Yield: 0.81 mmol (83%); buff-white solid; mp 156–158 °C; R_f 0.57.

FTIR (neat): 3181, 3003, 1753, 1644, 1604, 1571, 1511, 1459, 1420, 1364, 1332, 1262, 1200, 1166, 1144, 1075, 1031, 1000, 959, 865, 820, 794, 766, 729, 699, 629 cm^{-1}.

^{1}H NMR (300 MHz, $CDCl_3$): δ = 9.533 (bs, NH), 7.690 (s, CH=N), 7.429–6.792 (m, 7 H, Ar-H), 4.749 (s, 2 H, O-CH_2-CO), 4.029 (s, 2 H, CO-CH_2-Ar), 3.955 (s, 3 H, OCH_3), 3.811 (s, 3 H, OCH_3), 3.793 (s, 3 H, OCH_3).

Anal. Calcd. for $C_{20}H_{22}N_2O_6$: C, 62.17; H, 5.74; N, 7.25; O, 24.84. Found: C, 60.12; H, 5.70; N, 7.17; O, 24.00.

(*E*)-*N*′-(4-(Allyloxy)-3-methoxybenzylidene)-2-(4-methoxyphenyl)acetohydrazide (3d)

Yield: 0.92 mmol (93%); white solid; mp 149–151 °C; R_f 0.59.

FTIR (neat): 3179, 3011, 1644, 1615, 1604, 1565, 1504, 1454, 1416, 1355, 1331, 1259, 1489, 1162, 1141, 1071, 1001, 998, 951, 861, 817, 720, 694 cm^{-1}.

^{1}H NMR (300 MHz, $CDCl_3$): δ = 9.714 (bs, NH), 7.700 (s, CH=N), 7.397–6.821 (m, 7 H, Ar-H), 6.121–6.046 (m, 1 H, =CH), 5.460–5.307 (m, 2 H, $=CH_2$), 4.668 (d, 2 H, O-CH_2-CH=), 4.032 (s, 2 H, CO-CH_2-Ar), 3.943 (s, 3 H, OCH_3), 3.767 (s, 3 H, OCH_3).

Anal. Calcd. for $C_{20}H_{22}N_2O_4$: C, 67.78; H, 6.26; N, 7.90; O, 18.06. Found: C, 61.63; H, 5.18; N, 7.55; O, 18.12.

Isopropyl (*E*)-2-(2-Methoxy-4-((2-(2-(4-methoxyphenyl)acetyl)hydrazono)methyl)phenoxy)acetate (3e)

Yield: 0.73 mmol (74%); white solid; mp 127–129 °C; R_f 0.63.

FTIR (neat): 3182, 3002, 1754, 1644, 1604, 1567, 1511, 1460, 1420, 1362, 1333, 1316, 1305, 1283, 1263, 1242, 1223, 1210, 1199, 1160, 1145, 1108, 1072, 1030, 999, 959, 865, 819, 793, 749, 729, 698, 628 cm^{-1}.

^{1}H NMR (300 MHz, $CDCl_3$): δ = 9.810 (bs, NH), 7.705 (s, CH=N), 7.405–6.729 (m, 7 H, Ar-H), 5.180–5.096 (m, 1 H, OCH), 4.698 (s, 2 H, O-CH_2-CO), 4.029 (s, 2 H, CO-CH_2-Ar), 3.949 (s, 3 H, OCH_3), 3.794 (s, 3 H, OCH_3), 1.259 (d, 6 H, $2CH_3$).

Anal. Calcd. for $C_{22}H_{26}N_2O_6$: C, 63.76; H, 6.32; N, 6.76; O, 23.16. Found: C, 61.98; H, 5.00; N, 6.71; O, 23.09.

(*E*)-*N*′-(4-(Benzyloxy)-3-methoxybenzylidene)-2-(4-methoxyphenyl)acetohydrazide (3f)

Yield: 0.83 mmol (86%); white solid; mp 151–153 °C; R_f 0.68.

FTIR (neat): 3192, 3035, 1648, 1604, 1569, 1510, 1458, 1421, 1369, 1332, 1316, 1306, 1264, 1229, 1200, 1182, 1169, 1142, 1073, 1032, 1011, 960, 903, 864, 845, 818, 800, 792, 736, 692, 653, 625 cm^{-1}.

^{1}H NMR (300 MHz, $CDCl_3$): δ = 9.444 (bs, NH), 7.664 (s, CH=N), 7.454–7.220 (m, 8 H, Ar-H), 7.010–6.803 (m, 4 H, Ar-H), 5.203 (s, 2 H, O-CH_2-CO), 4.023 (s, 2 H, CO-CH_2-Ar), 3.973 (s, 3 H, OCH_3), 3.814 (s, 3 H, OCH_3).

Anal. Calcd. for $C_{24}H_{24}N_2O_4$: C, 71.27; H, 5.98; N, 6.93; O, 15.82. Found: C, 68.13; H, 5.00; N, 6.78; O, 14.96.

(*E*)-2-Methoxy-4-((2-(2-(4-methoxyphenyl)acetyl)hydrazono)methyl)phenyl Acetate (3g)

Yield: 0.71 mmol (71%); white solid; mp 174–176 °C; R_f 0.47.

FTIR (neat): 3189, 3010, 1768, 1649, 1606, 1569, 1510, 1460, 1416, 1368, 1317, 1268, 1245, 1200, 1162, 1139, 1075, 1031, 1013, 1002, 959, 944, 900, 863, 824, 793, 751, 730, 692, 667, 629 cm^{-1}.

^{1}H NMR (300 MHz, $CDCl_3$): δ = 9.445 (bs, NH), 7.705 (s, CH=N), 7.341–6.837 (m, 7 H, Ar-H), 4.028 (s, 2 H, CO-CH_2-Ar), 3.897 (s, 3 H, OCH_3), 3.801 (s, 3 H, OCH_3), 2.339 (s, 3 H, CO-CH_3).

Anal. Calcd. for $C_{19}H_{20}N_2O_5$: C, 64.04; H, 5.66; N, 7.86; O, 22.45. Found: C, 62.01; H, 5.40; N, 7.55; O, 22.32.

Methyl (*E*)-2-(4-((2-(2-(4-Methoxyphenyl)acetyl)hydrazono)methyl)phenoxy)acetate (3h)

Yield: 0.69 mmol (69%); white solid; mp 119–121 °C; R_f 0.59.

FTIR (neat): 3230, 3049, 1759, 1655, 1606, 1547, 1511, 1435, 1419, 1367, 1346, 1302, 1243, 1210, 1169, 1081, 1029, 989, 960, 871, 831, 815, 776, 738, 715, 690 cm^{-1}.

^{1}H NMR (300 MHz, $CDCl_3$): δ = 9.739 (bs, NH), 7.718 (s, CH=N), 7.620 (d, 2 H, Ar-H), 7.309–7.728 (dd, 2 H, Ar-H), 6.952–6.832 (m, 4 H, Ar-H), 4.685 (s, 2 H, O-CH_2-CO), 4.017 (s, 2 H, CO-CH_2-Ar), 3.825 (s, 3 H, OCH_3), 3.767 (s, 3 H, OCH_3).

Anal. Calcd. for $C_{19}H_{20}N_2O_5$: C, 64.04; H, 5.66; N, 7.86; O, 22.45. Found: C, 64.00; H, 5.54; N, 7.79; O, 22.42.

(*E*)-*N*′-(4-((2-Chlorobenzyl)oxy)benzylidene)-2-(4-methoxyphenyl)acetohydrazide (3i)

Yield: 0.74 mmol (76%); white solid; mp 172–174 °C; R_f 0.73.

FTIR (neat): 3191, 3037, 1654, 1608, 1553, 1512, 1457, 1420, 1382, 1344, 1304, 1236, 1200, 1172, 1078, 1035, 1026, 989, 842, 873, 838, 821, 779, 742, 704, 683, 640 cm^{-1}.

^{1}H NMR (300 MHz, $CDCl_3$): δ = 9.334 (bs, NH), 7.701 (s, CH=N), 7.645–7.226 (m, 8 H, Ar-H), 7.039–6.836 (m, 4 H, Ar-H), 5.218 (s, 2 H, O-CH_2-CO), 4.021 (s, 2 H, CO-CH_2-Ar), 3.771 (s, 3 H, OCH_3).

Anal. Calcd. for $C_{23}H_{21}ClN_2O_3$: C, 67.56; H, 5.18; N, 6.85; O, 11.74. Found: C, 61.33; H, 4.76; N, 6.80; O, 11.61.

(*E*)-2-(4-Methoxyphenyl)-*N*′-(4-(3-methoxypropoxy)benzylidene)acetohydrazide (3j)

Yield: 0.63 mmol (65%); white solid; mp 118–120 °C; R_f 0.72.

FTIR (neat): 3184, 3035, 1661, 1605, 1552, 1505, 1467, 1427, 1387, 1345, 1299, 1241, 1168, 1130, 1091, 1060, 1022, 954, 929, 898, 819, 803, 778, 751, 713, 680 cm^{-1}.

^{1}H NMR (300 MHz, $CDCl_3$): δ = 9.713 (bs, NH), 7.715 (s, CH=N), 7.700 (d, 2 H, Ar-H), 7.317–7.220 (dd, 2 H, Ar-H), 6.946–6.830 (m, 4 H, Ar-H), 4.023 (s, 2 H, CO-CH_2-Ar), 3.811 (s, 3 H, OCH_3), 3.765 (s, 3 H, OCH_3), 3.568 (t, 2 H, OCH_2), 3.355 (t, 2 H, OCH_2), 2.070 (m, 2 H, C-CH_2).

Anal. Calcd. for $C_{20}H_{24}N_2O_4$: C, 67.40; H, 6.79; N, 7.86; O, 17.96. Found: C, 62.76; H, 6.03; N, 7.35; O, 17.91.

Conflict of Interest

The authors declare no conflict of interest.

Funding Information

S.M. is thankful to the Head of the Department of Pharmaceutical Sciences & Technology, Birla Institute of Technology, Mesra for the provision of IRF (2022–2023; Ref. DPGS/Ph.D/IRF/2022-23/15, DATED 16-08-2022), from the Birla Institute of Technology, Mesra.

Acknowledgment

S.M. and A.P. thank the doctoral committee formed for the Ph.D. topic of S.M. The authors also extend their gratitude to the CIF facility, BIT, Mesra, India for provision of elemental and mass analysis.

Supporting Information

Supporting information for this article is available online at https://doi.org/10.1055/a-2035-6493.

References

(1) Popiołek, Ł. *Med. Chem. Res.* **2017**, *26*, 287.
(2) Popiołek, Ł. *Int. J. Mol. Sci.* **2021**, *22*, 9389.
(3) Mali, S. N.; Thorat, B. R.; Gupta, D. R.; Pandey, A. *Eng. Proc.* **2021**, *11*, 21.
(4) Thiyagarajan, S.; Gunanathan, C. *Org. Lett.* **2020**, *22*, 6617.
(5) DeMarinis, R. M.; Hoover, J. R. E.; Dunn, G. L.; Actor, P.; Uri, J. V.; Weisbach, J. *J. Antibiot.* **1975**, *28*, 463.
(6) Elnagdi, M. H.; Erian, A. W. *Arch. Pharm.* **1991**, *324*, 853.

(7) Costales, M. J.; Kleschick, W. A.; Ehr, R. J.; Weimer, M. R. US Patent 5,763,359, 9 June, **1998**.
(8) Gemma, S.; Kukreja, G.; Fattorusso, C.; Persico, M.; Romano, M. P.; Altarelli, M.; Savini, L.; Campiani, G.; Fattorusso, E.; Basilico, N. *Bioorg. Med. Chem. Lett.* **2006**, *16*, 5384.
(9) Bijev, A. *Lett. Drug Des. Discovery* **2006**, *3*, 506.
(10) Ragavendran, J. V.; Sriram, D.; Patel, S. K.; Reddy, I. V.; Bharathwajan, N.; Stables, J.; Yogeeswari, P. *Eur. J. Med. Chem.* **2007**, *42*, 146.
(11) Todeschini, A. R.; de Miranda, A. L. P.; da Silva, K. C. M.; Parrini, S. C.; Barreiro, E. J. *Eur. J. Med. Chem.* **1998**, *33*, 189.
(12) Ergenç, N.; Günay, N. S.; Demirdamar, R. *Eur. J. Med. Chem.* **1998**, *33*, 143.
(13) Deep, A.; Jain, S.; Sharma, P. C.; Verma, P.; Kumar, M.; Dora, C. P. *Synthesis* **2010**, 183.
(14) Masunari, A.; Tavares, L. C. *Bioorg. Med. Chem.* **2007**, *15*, 4229.
(15) Fahmy, S. M.; Badran, A. H.; Elnagdi, M. H. *J. Chem. Technol. Biotechnol.* **1980**, *30*, 390.
(16) Abdel-Wahab, B. F.; Awad, G. E.; Badria, F. A. *Eur. J. Med. Chem.* **2011**, *46*, 1505.
(17) Palekar, V. S.; Damle, A. J.; Shukla, S. R. *Eur. J. Med. Chem.* **2009**, *44*, 5112.
(18) Zhong, N. J.; Wang, Y. Z.; Cheng, L. *Org. Biomol. Chem.* **2018**, *16*, 5214.
(19) Özkay, Y.; Tunalı, Y.; Karaca, H.; Işıkdağ, İ. *Eur. J. Med. Chem.* **2010**, *45*, 3293.
(20) Abdel-Aziz, H. A.; Mekawey, A. A. *Eur. J. Med. Chem.* **2009**, *44*, 4985.
(21) Verma, G.; Marella, A.; Shaquiquzzaman, M.; Akhtar, M.; Ali, M. R.; Alam, M. M. *J. Pharm. Bioallied Sci.* **2014**, *6*, 69.
(22) Küçükgüzel, Ş. G.; Oruç, E. E.; Rollas, S.; Şahin, F.; Özbek, A. *Eur. J. Med. Chem.* **2002**, *37*, 197.
(23) Asif, M. *Int. J. Adv. Chem.* **2014**, *2*, 85.
(24) Rollas, S.; Gulerman, N.; Erdeniz, H. *Farmaco* **2002**, *57*, 171.
(25) Jubie, S.; Meena, S.; Ramaseshu, K. V.; Jawahar, N.; Vijayakumar, S. *Indian J. Chem.* **2010**, *49*, 1261.
(26) Govindasami, T.; Pandey, A.; Palanivelu, N.; Pandey, A. *Int. J. Org. Chem.* **2011**, *1*, 71.
(27) Tavares, L. C.; Chiste, J. J.; Santos, M. G.; Penna, T. C. II. *Boll. Chim. Farm.* **1999**, *138*, 432.
(28) Ulusoy, N.; Çapan, G.; Otük, G.; Kiraz, M. *Boll. Chim. Farm.* **2000**, *139*, 167.
(29) Szmant, H. H.; McGinnis, C. *J. Am. Chem. Soc.* **1950**, *72*, 2890.
(30) Kiasat, A. R.; Kazemi, F.; Nourbakhsh, K. *Phosphorus, Sulfur Silicon Relat. Elem.* **2004**, *179*, 569.
(31) Polshettiwar, V.; Varma, R. S. *Tetrahedron Lett.* **2007**, *48*, 5649.
(32) Chakraborti, A. K.; Bhagat, S.; Rudrawar, S. *Tetrahedron Lett.* **2004**, *45*, 7641.
(33) Lalitha, A.; Pitchumani, K.; Srinivasan, C. *Green Chem.* **1999**, *1*, 173.
(34) Niknam, K.; Kiasat, A. R.; Karimi, S. *Synth. Commun.* **2005**, *35*, 2231.
(35) Yadav, U. N.; Shankarling, G. S. *J. Mol. Liq.* **2014**, *191*, 137.
(36) Parveen, M.; Azaz, S.; Malla, A. M.; Ahmad, F.; da Silva, P. S. P.; Silva, M. R. *New J. Chem.* **2015**, *39*, 469.
(37) (a) Jarikote, D. V.; Deshmukh, R. R.; Rajagopal, R.; Lahoti, R. J.; Daniel, T.; Srinivasan, K. V. *Ultrason. Sonochem.* **2003**, *10*, 45. (b) Lima Leite, A. C.; Moreira, D. R. d. M.; Duarte Coelho, L. C.; de Menezes, F. D.; Brondani, D. J. *Tetrahedron Lett.* **2008**, *49*, 1538.
(38) Gadhwal, S.; Baruah, M.; Sandhu, J. S. *Synlett* **1999**, 1573.
(39) Zhang, M.; Shang, Z. R.; Li, X. T.; Zhang, J. N.; Wang, Y.; Li, K.; Li, Y. Y.; Zhang, Z. H. *Synth. Commun.* **2017**, *47*, 178.
(40) Shelke, P. B.; Mali, S. N.; Chaudhari, H. K.; Pratap, A. P. *J. Heterocycl. Chem.* **2019**, *56*, 3048.
(41) Mali, S. N.; Pandey, A. *Curr. Comput.-Aided Drug Des.* **2022**, *25*, 771.
(42) Bhosale, D.; Mali, S. N.; Thorat, B. R.; Wavhal, S. S.; Bhagat, D. S.; Borade, R. M. *Recent Pat. Anti-Infect. Drug Discovery* **2022**, *17*, 69.
(43) Mali, S. N.; Pandey, A. *J. Comput. Biophys. Chem.* **2022**, *21*, 857.
(44) Desale, V. J.; Mali, S. N.; Thorat, B. R.; Yamgar, R. S. *Curr. Comput.-Aided Drug Des.* **2021**, *17*, 493.
(45) Thorat, B. R.; Mali, S. N.; Rani, D.; Yamgar, R. S. *Curr. Comput.-Aided Drug Des.* **2021**, *17*, 294.
(46) Mali, S. N.; Pandey, A.; Thorat, B. R.; Lai, C.-H. *Chem. Proc.* **2022**, *8*, 86.
(47) Desale, V. J.; Mali, S. N.; Chaudhari, H. K.; Mali, M. C.; Thorat, B. R.; Yamgar, R. S. *Curr. Comput.-Aided Drug Des.* **2020**, *16*, 618.
(48) Thorat, B. R.; Rani, D.; Yamgar, R. S.; Mali, S. N. *Comb. Chem. High Throughput Screening* **2020**, *23*, 392.
(49) Mishra, V. R.; Ghanavatkar, C. W.; Mali, S. N.; Qureshi, S. I.; Chaudhari, H. K.; Sekar, N. *Comput. Biol. Chem.* **2019**, *78*, 330.
(50) Mali, S. N.; Pandey, A. *J. Comput. Biophys. Chem.* **2022**, *21*, 83.
(51) Kapale, S. S.; Mali, S. N.; Chaudhari, H. K. *Med. Drug Discovery* **2019**, *2*, 100008.
(52) Kshatriya, R.; Shelke, P.; Mali, S.; Yashwantrao, G.; Pratap, A.; Saha, S. *ChemistrySelect* **2021**, *6*, 6230.
(53) Mali, S. N.; Pandey, A.; Thorat, B. R.; Lai, C. H. *Struct. Chem.* **2022**, *33*, 679.
(54) Mali, S. N.; Pandey, A. *J. Indian Chem. Soc.* **2021**, *98*, 100082.
(55) Mali, S. N.; Pandey, A.; Bhandare, R. R.; Shaik, A. B. *Sci. Rep.* **2022**, *12*, 16368.
(56) Yang, H.; Lou, C.; Sun, L.; Li, J.; Cai, Y.; Wang, Z.; Li, W.; Liu, G.; Tang, Y. *Bioinformatics* **2019**, *35*, 1067.
(57) Ioakimidis, L.; Thoukydidis, L.; Mirza, A.; Naeem, S.; Reynisson, J. *QSAR Comb. Sci.* **2008**, *27*, 445.
(58) Parveen, M.; Azaz, S.; Malla, A. M.; Ahmad, F.; da Silva, P. S. P.; Silva, M. R. *New J. Chem.* **2015**, *39*, 469.